International Journal of Biological Macromolecules 254 (2024) 127909

Contents lists available at ScienceDirect

International Journal of Biological Macromolecules

journal homepage: www.elsevier.com/locate/ijbiomac

Design, synthesis and anticancer evaluation of novel arylhydrazones of active methylene compounds

Akshaya Murugesan [a,b], Saravanan Konda Mani [c], Shabnaz Koochakkhani [b], Kumar Subramanian [d], Jayalakshmi Kandhavelu [d], Ramesh Thiyagarajan [e], Atash V. Gurbanov [f,g], Kamran T. Mahmudov [f,g], Meenakshisundaram Kandhavelu [b,*]

[a] Department of Biotechnology, Lady Doak College, Madurai Kamaraj University, Thallakulam, Madurai 625002, India
[b] Molecular Signaling Group, Faculty of Medicine and Health Technology, Tampere University and BioMediTech, P.O. Box 553, 33101 Tampere, Finland
[c] Department of Biotechnology, Bharath Institute of Higher Education & Research, Chennai 600 073, Tamilnadu, India
[d] Oncology Division, Faculty of Health Sciences, University of the Witwatersrand, Parktown, Johannesburg, South Africa
[e] Department of Basic Medical Sciences, College of Medicine, Prince Sattam Bin Abdulaziz University, Al-Kharj 11942, Saudi Arabia
[f] Centro de Química Estrutural, Institute of Molecular Sciences, Instituto Superior Técnico, Universidade de Lisboa, Av. Rovisco Pais, 1049-001 Lisboa, Portugal
[g] Excellence Center, Baku State University, Z. Xalilov Str. 23, Az 1148 Baku, Azerbaijan

ARTICLE INFO

Keywords:
Glioblastoma
Molecular docking
TrkA inhibitor
Hydrazone derivatives

ABSTRACT

Nerve growth factor (NGF) and its receptor, tropomyosin kinase receptor kinase type A (TrkA) is emerging as an important target for Glioblastoma (GBM) treatment. TrkA is the cancer biomarker majorly involved in tumor invasion and migration into nearby normal tissue. However, currently, available Trk inhibitors exhibit many adverse effects in cancer patients, thus demanding a novel class of ligands to regulate Trk signaling. Here, we exploited the role of TrkA (NTRK1) expression from the 651 datasets of brain tumors. RNA sequence analysis identified overexpression of NTRK1 in GBM, recurrent GBM as well in Oligoastrocytoma patients. Also, TrkA expression tends to increase over the higher grades of GBM. TrkA protein targeting hydrazone derivatives, R48, R142, and R234, were designed and their mode of interaction was studied using molecular docking and dynamic simulation studies. Ligands' stability and binding assessment reveals R48, 2 2-(2-(2-hydroxy-4-nitrophenyl) hydrazineylidene)-1-phenylbutane-1,3-dione, as a potent ligand that interacts well with TrkA's hydrophobic residues, Ile, Phe, Leu, Ala, and Val. R48- TrkA exhibits stable binding potentials with an average RMSD value <0.8 nm. R48 obeyed Lipinski's rule of five and possessed the best oral bioavailability, suggesting R48 as a potential compound with drug-likeness properties. In-vitro analysis also revealed that R48 exhibited a higher cytotoxicity effect for U87 GBM cells than TMZ with the IC_{50} value of 68.99 μM. It showed the lowest percentage of cytotoxicity to the non-cancerous TrkA expressing MEF cells. However, further SiRNA analysis validates the non-specific binding of R48, necessitating structural alteration for the development of R48-based TrkA inhibitor for GBM therapeutics.

1. Introduction

Glioblastoma or Glioblastoma multiforme (GBM) is one of the most common malignant brain tumors, characterized with aberrant activation of numerous signal transduction pathways [1,2]. Among several proteins involved in key signaling pathways, receptor tyrosine kinases (RTKs) family proteins exerts crucial connections with many pathways by regulating angiogenesis, invasion, migration, proliferation, and apoptosis [3].The RTKs family embraces several sub-families including the epidermal growth factor receptors (EGFRs or ERBBs), the fibroblast growth factor receptors (FGFRs), the insulin and the insulin-like growth factor receptors (IR and IGFR), the platelet-derived growth factor receptors (PDGFRs), the vascular endothelial growth factor receptors (VEGFRs), the hepatocyte growth factor receptors (HGFRs), and the nerve growth factor receptors (NGFRs) [4]. The crucial and diverse roles of RTKs are evident not only in GBM prognosis, but also in many other cancers that occur due to gain-of-function in RTK signaling [5,6].

Nerve growth factor (NGF), a member of the neurotrophin family,

* Corresponding author.
E-mail address: meenakshisundaram.kandhavelu@tuni.fi (M. Kandhavelu).

https://doi.org/10.1016/j.ijbiomac.2023.127909
Received 31 May 2023; Received in revised form 2 November 2023; Accepted 3 November 2023
Available online 10 November 2023

has thriving roles in mitogenesis of GBM cells via interaction with tropomyosin receptor kinase (Trk), also known as NGFR [7]. NGF might epitomize an ideal aspirant therapeutic molecule for GBM, because it has been characterized as a factor inducing differentiated, post-mitotic state in neurons [8]. Notably, Trk member proteins, TrkA, TrkB, and TrkC overexpressed in GBM cells [9]. NGF exerts its biological effect by binding to the high affinity tyrosine kinase (TrkA, p140TrkA, and gp140TrkA) [10,11]. NGFR, which in turn activates its cytoplasmic tyrosine kinase domain and causes a rapid increase in phosphorylation of cellular substrates. The activation of different neurotrophin–Trk systems can inhibit tumor cell growth [12]. The higher malignancy property of squamous carcinomas is associated with both increased proliferative activity and reduction in the rate of apoptosis [13].

According to the cancer genome atlas (TCGA) program, RTK signaling pathways were found to be the most commonly altered core signaling pathways in approximately 90 % of GBM tumors [14]. GBM was the first cancer type to be systemically analyzed using genomic approaches. It is important to mention that the EGFR family is a central target for the most prevalent genetic RTK mutations. GBM frequently has alterations in the PDGFR and MET tyrosine kinase pathways, resulting in the development of therapies targeting these RTKs for treatment [15]. Although there are several RTK inhibitors in clinical trials, their efficacy in treating GBM is still restricted. In recent literature reviews, there has been significant discussion about the genetic changes of RTK in the development of glioma, the primary targets of RTK in GBM, and the potential and limitations of targeted treatment [15,16].

Notably, the RTKs signal regulates two major downstream pathways Raf/MAPK/ERK 1\2 and Ras/PI3K/AKT, which plays crucial role in tumor angiogenesis [17]. TRK inhibitors have shown potential activity against the growth of TrkB over expressing neuroblastoma cells. Clinically tested TRK inhibitor lestaurtinib, otherwise called as CEP-701/KT-5555, have shown limited effect on the patients diagnosed neuroblastoma [18]. Thus, it is necessary to identify patients specific TRK inhibitor or potential targeted TRK inhibitor for the patients expressing TrkA, TrkB, and TrkC. Recently, we have synthesized 23 arylhydrazones of active methylene compounds (AHAMCs) and showed their molecular interaction with TrkA. One of the top compound, 2-(2-(2,4-dioxopentan-3-ylidene) hydrazineyl)benzonitrile) (R234) was identified as the potent derivative against the growth of glioblastoma cell [19]. The R234 was identified as multi-kinase inhibitor which reduced the GBM cell viability and proliferation in-vitro. It was shown to interrupt the cell cycle at G1/S phase, initiates apoptotic cell death via caspase 3/7 activation through the regulation of PI3K/AKT/mTOR signaling pathway in GBM. It is also noted that, hydrazones derivatives have shown diverse biological and pharmacological properties including antimicrobial, anti-inflammatory, analgesic, antifungal, anti-tubercular, antiviral, anticancer, antiplatelet, antimalarial, anticonvulsant, cardio protective, anthelmintic, anti-protozoal [20], anti-trypanosomal [21],) antischistosomiasis [22].

In the previous work, we established that hydrazone derivative, R234 as a TrkA inhibitor with higher anti-GBM potential. We also noticed that the compounds 2-(2-(2-hydroxy-4-nitrophenyl) hydrazineylidene)-1-phenylbutane-1,3-dione (R48) and 2-hydroxy-5-nitro-3-(2-(2,4,6-trioxotetrahydropyrimidin-5(2H)-ylidene)hydrazineyl)benzenesulfonic acid (R142) showed better interaction with the TrkA receptor than the other hydrazone derivatives [19]. Other research groups have also proven that hydrazone derivatives as a potential tyrosine kinase inhibitor with anticancerous effect [23,24]. The current study intends to correlate the pharmacodynamic of the two of the top hydrazone derivatives using Insilico and experimental approach. Specifically, here we built a theoretical TrkA structural model and studied the molecular interactions of structurally similar hydrazone derivatives including R48 and R142. The structure-based predictions of pharmacokinetic properties were also analyzed and the lead compound was synthesized for further evaluation. The effect of hydrazone derivatives against the GBM is also investigated to reveal their cytotoxicity potential. Thus, the findings of present study might open a new opportunity to develop a clinically potential compound as TrkA inhibitor for treating glioblastoma.

2. Experimental section

2.1. TrkA mRNA expression analysis

GlioVis (http://gliovis.bioinfo.cnio.es/), a publicly available web portal for data visualization and analysis of brain tumors was used to explore the expression datasets of TrkA (NTRK1). Totally, 651 datasets as on 28/01/2023 of brain tumors were analyzed using the personalized parameters of TrkA expression in primary and recurrent tumors of GBM including oligoastrocytoma, oligodendroglioma, astrocytoma, Anaplastic oligodendroglioma, anaplastic oligoastrocytoma and anaplastic astrocytoma. The difference in the expression level of TrkA among the several grades of glioblastoma was also analyzed and the processed log2-transformed intensities from the 651 GBM datasets were represented as the boxplots.

2.2. Molecular docking

The target protein structure for the Human Nerve Growth Factor Receptor TrkA's (PDB ID:1HE7) atomic coordinates was retrieved from the Research Collaboratory for Structural Bioinformatics (RCSB) Protein Data Bank [25], with the resolution of 2.00 Å [26]. Autodock 4.26 [27] was used for the preparation of crystal structure of the protein, where the PDB files was cleaned, missing side chains and loops were built, and the hydrogen bonds were optimized. Water molecules were also eliminated to clear the binding pockets that might confound and distort the pose search. The structure's energy was verified and optimized using OPLS 2005 force field [28]. This force field was used to add the hydrogen bonds and further to determine the bond length. The grid maps were obtained from the ligand-binding sites from the PDBsum. Autodock Vina [29] was used for the molecular docking where ten poses for each ligand was selected and saved for subsequent analysis [30]. The interactions between protein-arylhydrazone derivatives were plotted using the Discovery Studio visualizer 3.1 downloaded from www.accelerys.com.

2.3. Docking simulations

Molecular dynamics simulation was performed on the modeled protein-ligand (hydrazone derivatives) complexes to examine the stability and structural changes using the GROMACS 5.0 (RRID:SCR) [31]. The topology files necessary for hydrogen atoms and ions were assigned using the AMBER99SB-ILDN force field together with the correct geometrical parameters [32]. The ionizable atoms' protonation state was chosen that correspond to pH 7.0, and the particle-mesh Ewald (PME) technique was used to calculate the potential energy [33]. The protein-ligand complexes were submerged in water, and the entire system was subjected to the steepest descent minimization with a maximum number of 50,000 steps to reduce energy consumption [34]. In the conventional NVT ensemble, the system was heated to 300 K in 100 ps using the Berendsen thermostat, and then 100 ps of Parrinello-Rahman pressure coupling was applied in the NPT ensemble [35]. Using the Leap-frog technique, the manufacturing molecular dynamics simulations were integrated for 40 ns, while all position restraints were removed. The whole set of simulations was run at two distinct temperatures: thermophilic 320 K and mesophilic 300 K [36]. The GROMACS software package's standard algorithms and analysis tools were used to analyze the data.

2.4. In-silico pharmacokinetics analysis and ADME/Tox prediction

To understand the fate of pharmacokinetics and ADME/Tox, predication of several parameters was done using the online available

SwissADME software (http://www.swissadme.ch/) (Daina et al., 2017). Additionally, small molecule pharmacokinetic properties using SMILES notation (https://biosig.lab.uq.edu.au/pkcsm/prediction) (accessed, March 2023) were performed by resorting to pkCSM [37]. The Lipinski violations and bioavailability score was determined in predicting the drug likeness of the all the compounds under investigation. Physiochemical properties (HBA/HBD, TPSA), lipophilicity, water solubility, human intestinal absorption (HIA), blood brain barrier (logBB) permeability was also determined. Metabolism of the hydrazone derivatives was also predicted based on the CYP models for substrate or inhibition such as CP1A2, CYP2C19, CYP2C9, CYP2D6, and CYP3A4.

2.5. Synthesis of novel arylhydrazone derivatives

The hydrazones R48, R142 and R234 were synthesized via Japp–-Klingemann reaction [38–40]. The detailed scheme of synthesis of R142 and R234 compounds are given in the supplemental file, where R234 was used as a control compound.

R48: yield 63 % (based on benzoylacetone), dark brown powder soluble in DMSO, methanol, ethanol and acetone, and insoluble in water. Elemental analysis: $C_{16}H_{13}N_3O_5$ (M = 327.3); C 58.35 (calc. 58.72); H 4.09 (4.00); N 12.45 (12.84) %. IR (KBr): 3442 ν(OH), 3184 ν(NH), 1624 ν(C═O), 1597 ν(C═O···H), 1527 ν(C═N) cm^{-1}. ^{1}H NMR of a mixture of hydrazone-I and hydrazone-II isomers in DMSO-d_6, internal TMS, hydrazone-I, δ (ppm): 2.23 (s, 3H, CH_3), 6.53–7.94 (5H, C_6H_5 and 3H, C_6H_3), 111.69 (s, 1H, HO–Ar), 13.08 (s, 1H, HO-enol). Hydrazone-II, δ: 2.18 (s, 3H, CH_3), 6.53–7.94 (5H, C_6H_5 and 3H, C_6H_3), 11.69 (s, 1H, HO–Ar), 14.13 (s, 1H, NH). ^{13}C{^{1}H} NMR (100.61 MHz, DMSO-d_6). Hydrazone-I, δ: 25.5 (CH_3), 110.0 (C—N), 110.2 (Ar—NH—N), 113.8, 116.3, 128.1, 128.6, 128.9, 132.6, 133.6 and 136.1 (Ar—H), 137.5 (Ar—CO), 142.8 (Ar—NO_2), 145.2 (Ar—OH), 191.5 (C═O), 192.7 (C═O). Hydrazo-II, δ: 30.2 (CH_3), 113.6, 116.3, 126.9, 128.5, 128.8, 130.3 and 132.7 (Ar—H), 135.2 (Ar—NH—N), 135.8 (Ar—H), 137.1 (C═N), 138.8 (Ar—CO), 143.4 (Ar—NO_2), 145.6 (Ar—OH), 196.4 and 197.6 (C═O).

R142: yield, 62 % (based on barbituric acid), yellow powder, soluble in water, methanol, ethanol, and insoluble in chloroform. Anal. Calcd for $C_{10}H_7N_5O_9S$ (M = 373.25): C, 32.18; H, 1.89; N, 18.76. Found: C, 32.12; H, 1.90; N, 18.58 %. IR, cm^{-1}: 3487 ν(OH), 3399, 3043, 2834 ν(NH), 1712 ν(C═O), 1655 ν(C═O), 1590 ν(C═O···H), 1560 ν(C═N). ^{1}H NMR (300.13 MHz, DMSO-d_6) δ: 8.10–8.30 (2H, C_6H_2), 11.42 (s, 1H, NH), 11.67 (s, 1H, NH) and 14.25 (s, 1H, NH). ^{13}C{^{1}H} NMR (100.61 MHz, DMSO-d_6) δ: 110.2 and 118.4 (2Ar—H), 120.6 (Ar—NH—N═), 130.4 (Ar—SO_3H), 131.4 (C═N), 139.9 (Ar—NO_2), 147.7 (Ar—OH), 149.8, 159.6 and 162.5 (C═O).

R234: yield 81 % (based on pentane-2,4-dione), yellow powder soluble in DMSO, methanol, ethanol, chloroform and acetone, and insoluble in water. Elemental analysis: $C_{12}H_{11}N_3O_2$ (M = 229); C 62.72 (calc. 62.87); H 4.85 (4.84); N 18.76 (18.33)%. IR (KBr): 3437 (NH), 2220 (C≡N), 1677 (C═O), 1639 (C═O···H), 1601 (C═N) cm^{-1}. ESI-MS: m/z: 230 $[M + H]^+$. ^{1}H NMR in DMSO-d_6, δ (ppm): 2.43 (s, 3H, free CH_3CO), 2.50 (s, 3H, CH_3CO in H-bond, overlapping with DMSO-d_6), 7.28–7.85 (4H, Ar—H), 14.35 (s, 1H, NAH). ^{13}C–{^{1}H} NMR in DMSO-d_6, δ (ppm): 26.60 (CH_3), 31.31 (CH_3), 99.01 (C≡N), 116.00 (Ar–CN), 116.13 (Ar—H), 125.08 (Ar—H), 133.48 (Ar—H), 134.98 (Ar—H), 135.19 (C═N), 143.94 (Ar–NH–N), 196.48 (C═O), 197.97 (C═O).

2.6. Cell line and culture condition

Glioblastoma cell, U-87 MG (gifted by Dr. Kirsi Rautajoki, Faculty of Medicine and Health Technology, Tampere) and mouse embryonic fibroblast cells, MEF cells (gifted by Prof. Pasi Kallio, Faculty of Medicine and Health Technology, Tampere) which overexpress TrkA receptor protein [41,42] were selected for the study. U-87 MG cell carries many mutations including the deletion of p14ARF and p16. It also expresses a wild type p53, tumor suppressor protein. MEF cell derived from E13.5 CF1 embryos. These cell lines were grown in Dulbecco's Modified Eagle Medium-high glucose (DMEM) (Biowest, #L0102-500), 1 % Penicillin, Streptomycin (Sigma-Aldrich, #P4333), 0.025 mg/ml Ampicillin B (Sigma-Aldrich, #A9528), 10 % Fetal Bovine Serum (FBS) (Biowest, #S181H-500). All the chemicals for the cell culture were purchased from Sigma-Aldrich (St. Louis, MO, USA). The cells were maintained in an aseptic humidified culture incubator at 37 °C supplemented with 5 % CO_2 and 95 % O_2. In-vitro experiments were performed with the cell passage number from 18 to 25 for both the cell lines.

2.7. Cytotoxicity assay of hydrazone derivatives

The cytotoxicity effect of hydrazone derivatives, R234, R48 and R142, was determined against the cell growth inhibition of U-87 MG and MEF cells. Firstly, the initial density of 1×10^5 cells/well of U-87 MG cells were seeded on a six-well plate and treated with 100 μM concentration of each derivative. Temozolomide (TMZ) was used as a drug control and 0.1 % DMSO as a negative control. The hydrazone derivatives, TMZ and 0.1 % DMSO (negative control) were incubated with the cells for 48 h. Treated cells were trypsinized and harvested by centrifugation at 153g for 10 min and pelleted cells were stained with trypan blue. The cells were loaded on a hemocytometer and the percentage of live and dead cells were measured using Countess II FL (Thermo Fisher Scientific, USA). The effect of all the tested conditions was assessed by quantifying the cell membrane integrity. However, MEF cells were treated with the 100 μM of the top lead hydrazone derivatives, TMZ and 0.1 % DMSO. The cytotoxic effect was measured as cell death percentage using the following Eq. (1).

$$\text{Cell growth inhibition}(\%) = \frac{Mean\ No.ofuntreated\ cells\ (DMSOcontrol) - Mean\ No.of\ treated\ cells}{Mean\ No.of\ untreated\ cells\ (DMSO\ control)} \times 100 \quad (1)$$

2.8. Dose dependent cell viability assay

The U-87 MG cells were seeded with the density of 1×10^5 cells/well in a 6 well plates and incubated for 24 h. The cells were then treated with different concentrations of hydrazone derivatives, R234, R48, R142 and TMZ (drug control) like 10 μM, 50 μM, 100 μM, 150 μM, and 200 μM concentrations. The DMSO (0.1 %) served as negative control. After 48 h post treatment, the cells were harvested by centrifugation at 153g for 10 min. The live and dead cells were stained using trypan blue [43] and were counted using Countess II FL hemocytometer (Thermo Fisher Scientific, USA). The percentage of cell growth inhibition was calculated using the above-mentioned Eq. (1). The half-maximal inhibitory concentrations (IC_{50}) of these compounds and TMZ were calculated using the dose response curve.

2.9. SiRNA assay

To validate the specificity of R48 binding with NTRK1, a SiRNA assay was performed using pre-designed SiRNA targeting NTRK1 (Thermo Fisher Scientific Inc. USA) (Cat no. AM16708). U-87 MG cells were

seeded in 12 well-plate at a density of 8×10^4 cells/well. The cells at a confluence of ≥80 % were transfected with SiRNA at a concentration of 50 nM using Mirus Bio™ TransIT-TKO™ SiRNA Transfection Reagent (Madison, WI, USA) (Cat no. MIR2154). Time series assay was performed by transfecting the cells for 24 h, 48 h, and 72 h, further treated with 200 μM concentration of R48 and maintained in culture condition for 48 h. Finally, the live and dead cells were calculated with the Eq. (1) using trypan blue assay.

2.10. Data and statistical analysis

Datapoints were represented as the mean ± S.E.M and the experiments were performed in triplicates with $n \geq 6$ per group. The one-way analysis of variance (ANOVA) was used to assess the statistical significance between different groups. Statistical significance values (*P*-value) for ANOVA corresponds to $^*P < 0.05$.

3. Result

3.1. TrkA is widely expressed in GBM

We have used 651 CGGA dataset from Gliovis to identify the expression hub for NTRK1 gene from different types of brain tumor. As a validation, we found that the expression level of TrkA was higher in GBM and oligoastrocytoma of both histological subtypes than the other brain tumor types (Fig. 1A). Also, the recurrence malignant GBM showed higher expression of TrkA than the other types (Fig. 1B). To classify the TrkA expression among different grades of GBM, we also stratified the expression for Grade II, III and IV. Grade IV showed pronounced expression of TrkA followed by grade III and II. These data revealed that TrkA expression gradually increases as the disease progresses from diffusive to infiltrative and finally to infiltrative rapid growing malignant tumor (Fig. 1C).

3.2. Hydrazone derivatives interaction with human receptor tyrosine kinase

To comprehend the potential binding affinity of human TrkA protein for the three different hydrazone derivates, R48, R142, and R234 (Fig. 2A) molecular docking was performed. The target protein 1HE7 co-crystallized with glycerol served as control for the point of comparison. The best docking score was computed using Autodock Vina and the binding energy of the protein-ligands was −7.62, −8.14, and −8.98 kcal/mol for R48, R142, and R234, respectively (Fig. 2B). The comparative analysis revealed that R48 had the highest binding affinity for TrkA with the maximum binding for the hydrophobic residues, Ile, Phe, Leu, Ala, and Val. Other two hydrazone derivates, R142 and R234 was also observed to interact best with TrkA protein, and thus considered as the potential TrkA inhibitors.

Further, we have investigated the protein-ligand complex interactions and stability of these three chosen complexes using atomic molecular dynamics simulations. Ligand induced alteration in the protein structure can be assessed through MD simulation. The root mean square deviation (RMSD) of the selected complexes reveals the stability of the protein-ligand complex. The minimal RMSD variation <0.5 nm suggest limited motion of the system, and in the Fig. 3A, it was identified that R234 exhibits stable throughout the simulation. Ligand R48 also remained stable throughout most of the simulation course, however, there observed considerable fluctuation >1. Overall, out of 40-ns simulation the RMSD value for R234 was found to be significantly low. The lesser RMSD values (>1 nm) show that reliable binding conformation was obtained throughout the simulation. Although there was a little fluctuation in the RMSD value, consistent binding still exists (R142). Mostly, protein-ligand interactions are often stabilized by hydrogen bonding, hydrophobic, and electrostatic interactions. Trajectory data was imported in the Gromacs tool to analyze the number of hydrogen bonds in terms of distance (3.5 Å) and HBD/HBA angle (30°) (Fig. 3B). R48 forms stable hydrogen bonds (>3) with the protein than the other two protein-ligand complexes maintaining the complex stability. Since, R48 appears to form relative number of stabilizing contacts, RMSD estimations and hydrogen bond numbers between protein and ligand support the conclusion that TrKA can form stable complex with R48.

3.3. Hydrazone derivatives possess ADMET properties

The investigation and optimization of pharmacokinetic properties of these three hydrazone derivates were performed using Swiss ADME web-based software and presented in the Table 1. Smiles were generated to perform the ADMET analysis. All the three hydrazone derivatives showed good water solubility. The intestinal absorption was effective and high for R48 and R234. According to the Lipinski rule of five (RO5), R48 and R234 have molecular weight <500 g/mol, topological polar surface area (TPSA) ≤ 140 Å, log *P* value <5 and hydrogen bond donor

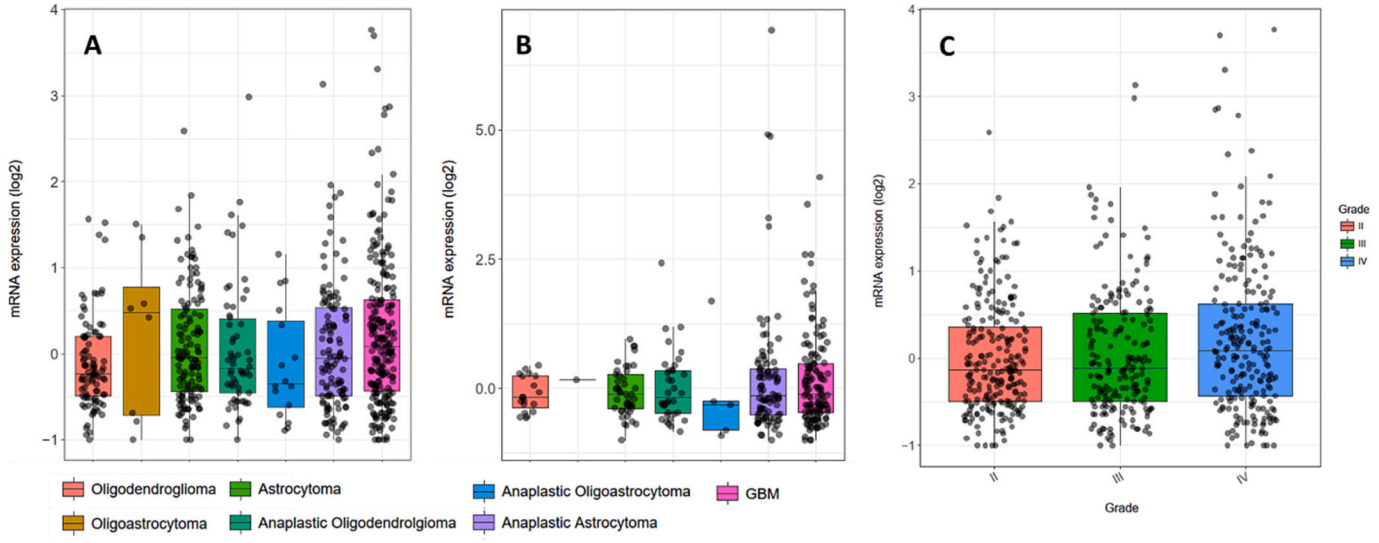

Fig. 1. TrkA as a biomarker in histological subtypes of GBM. (A) TrkA (NTRK1) expression profile across all primary tumor samples. (B) Recurring tumor samples (C) GBM grade II, III and IV from the CGGA dataset.

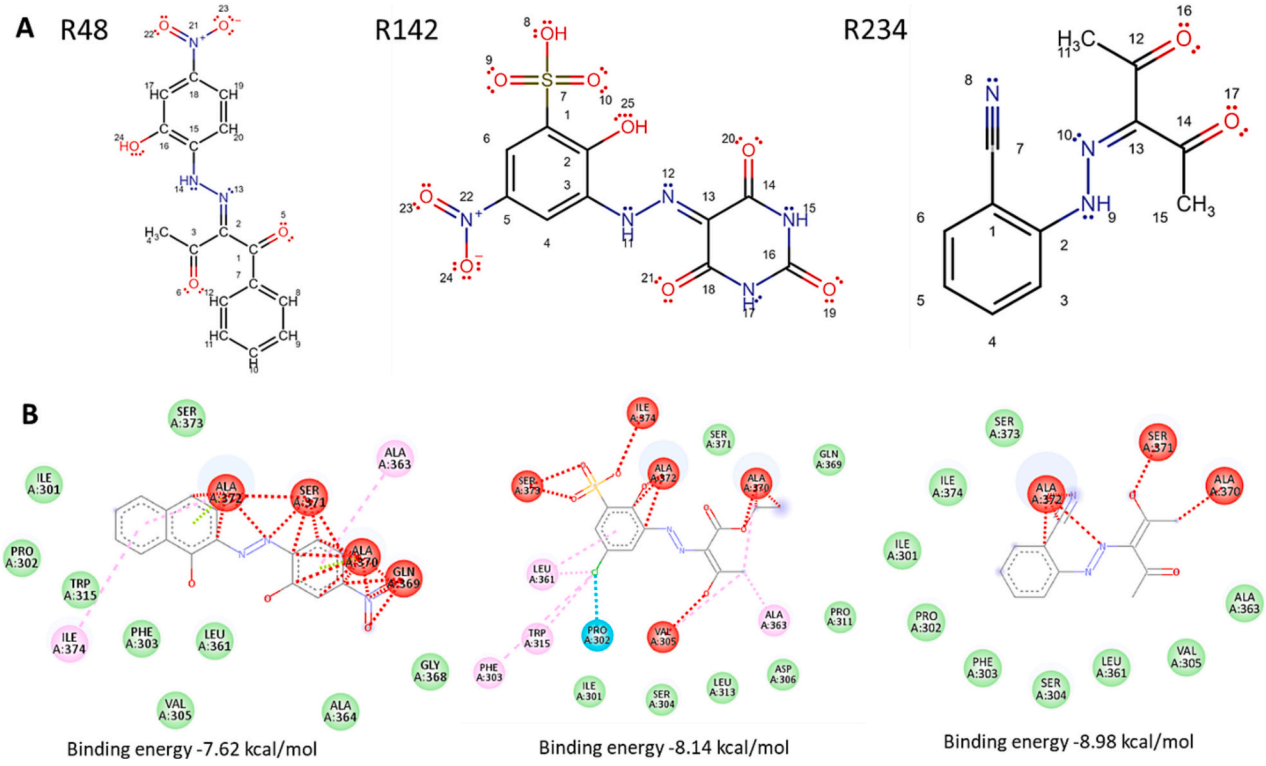

Fig. 2. Structure activity relationship of hydrazone derivatives: a) Structure of R48, R142 and R234 B) Interaction of R48, R142 and R234 with TrkA receptor.

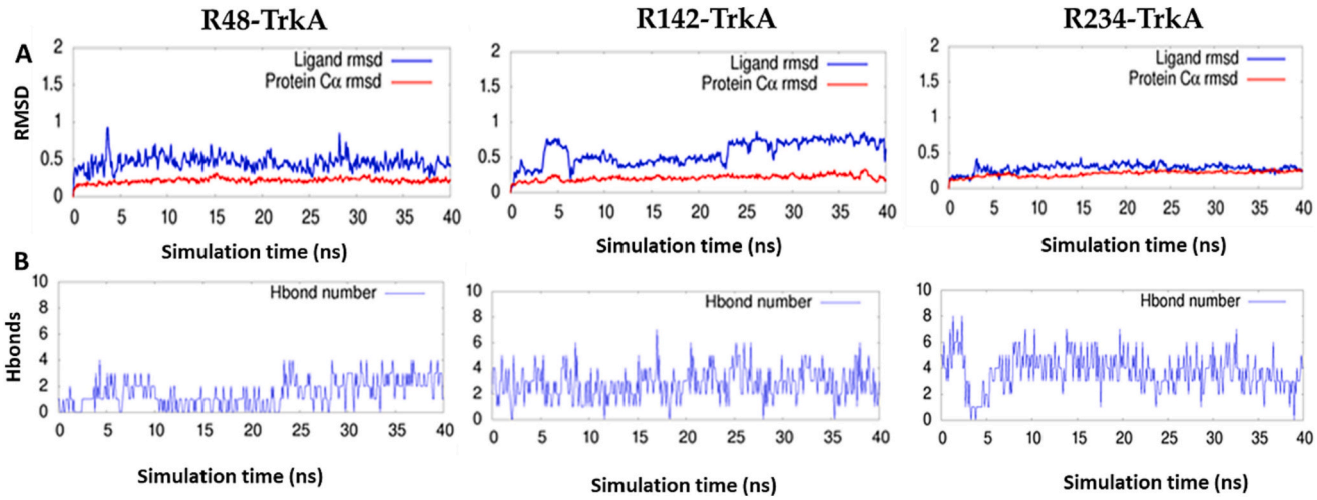

Fig. 3. Molecular dynamics simulation of hydrazone derivatives. A) The graph showing the RMSD data of all the ligand-protein complexes (R48, R142 and R234 interaction with TrkA receptor) at 40 ns duration of simulation. B) The graph representing the number of hydrogen bond interactions.

(HBD)/hydrogen bond acceptor (HBA) < 5/10. R48 is found to be an inhibitor of CYP2C9, a crucial feature for drug interaction and as well an indicator representing its metabolism in liver. Thus, out of all these three derivatives, R48 and R234 possess good distribution and excretion properties.

3.4. R48 targets TrkA expressing GBM cells

TrkA targeting hydrazone analogs, R48 was synthesized according to the scheme (Fig. 4) and synthesis of R142, and R234 were reported in the Supplemental file. Purity of all the derivatives were identified by the melting point, NMR data, elemental analysis and mass spectrometry measurements (Supplemental file). Cytotoxicity activity of the TrkA targeting hydrazones derivatives were carried out in TrkA expressing GBM cells with 100 μM concentration of R234, R48, R142 compounds (Fig. 5A). TMZ was used as the positive control and DMSO as the negative control. We have observed 53.5 %, 27.5 % and 44 % of cell growth inhibition for R48, R142 and R234, respectively. The highest cytotoxicity was noted for R48 followed by R234 and R142. Comparatively, all the three derivatives showed higher and significant cell death than the positive control, TMZ. To evaluate the IC_{50} concentration of all the derivatives, dose dependent cytotoxicity analysis of R234, R48, R142 in GBM cell line, U-87 MG was performed. Broader concentrations such as 10 μM, 50 μM, 100 μM, 150 μM and 200 μM concentration of hydrazone derivatives were chosen for the study. As the concentration increases, there observed an increased percentage of growth inhibition

Table 1
ADMET analysis showing pharmacokinetic properties of these three hydrazone derivates.

	Properties	R48	R234	R142
Physicochemical Properties	MW	327.29	229.23	373.26
	#H-bond acceptors	6	4	10
	#H-bond donors	2	1	5
	TPSA	124.58	82.32	228.46
Lipophilicity	iLOGP	0.99	1.85	-1.28
	XLOGP3	3.31	1.9	-0.09
	WLOGP	2.87	1.31	-0.67
	MLOGP	0.48	0.32	-2.57
	Silicos-IT Log P	0.87	1.91	-3.4
Water Solubility	Consensus Log P	1.71	1.46	-1.6
	ESOL Class	Soluble	Soluble	Soluble
	Ali Class	Moderately soluble	Soluble	Moderately soluble
	Silicos-IT class	Moderately soluble	Soluble	Soluble
Pharmacokinetics	GI absorption	High	High	Low
	BBB permeant	No	No	No
	Pgp substrate	No	No	Yes
	CYP1A2 inhibitor	No	Yes	No
	CYP2C19 inhibitor	No	No	No
	CYP2C9 inhibitor	Yes	No	No
	CYP2D6 inhibitor	No	No	No
	CYP3A4 inhibitor	No	No	No
	log Kp (cm/s)	-5.95	-6.35	-8.64
Druglikeness	Lipinski #violations	0	0	1
	Bioavailability Score	0.55	0.55	0.11
Medicinal Chemistry	PAINS #alerts	1	1	1

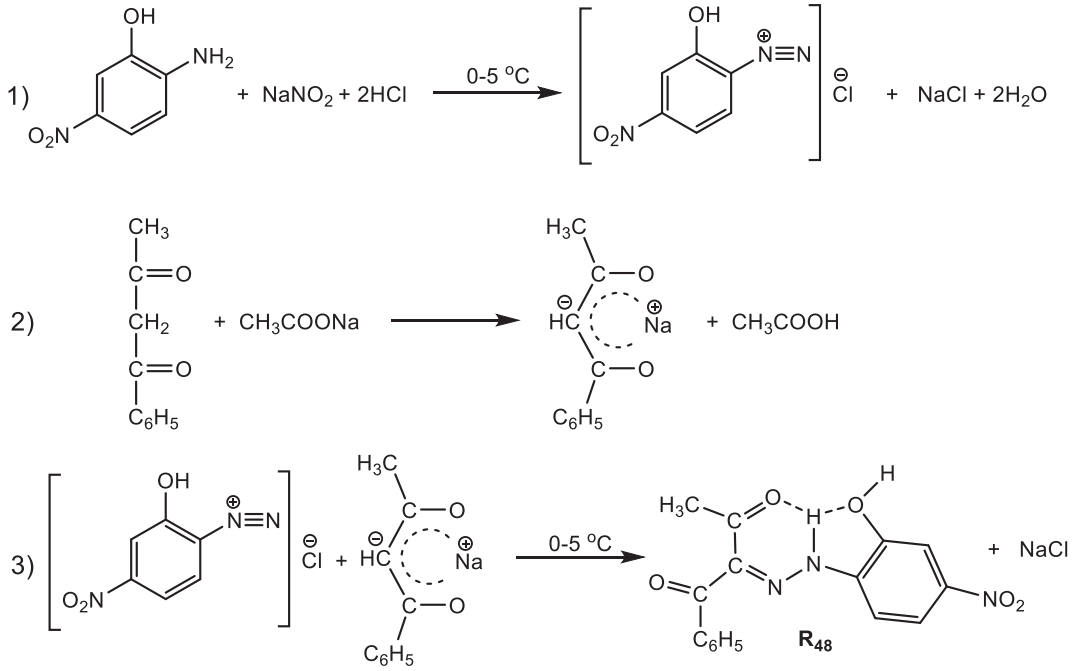

Fig. 4. Synthesis scheme of R48: Scheme shows the sequential steps of Japp-Klingemann synthesis of hydrazone analog R48. Synthesis scheme of R142 and R234 were reported in the supplementary file.

of GBM cells. The IC_{50} concentration of R48, R142 and R234 was found to be 68.99 μM, 125 μM and 106 μM, respectively (Fig. 5B). It was well correlated with the previous in-silico data, that R48 found to exhibit higher cytotoxicity effect after 48 h of treatment in U-87 MG cells. Phase-contrast microscopic images also revealed the presence of cellular structural changes with shrunken cell population in R48 treated cells

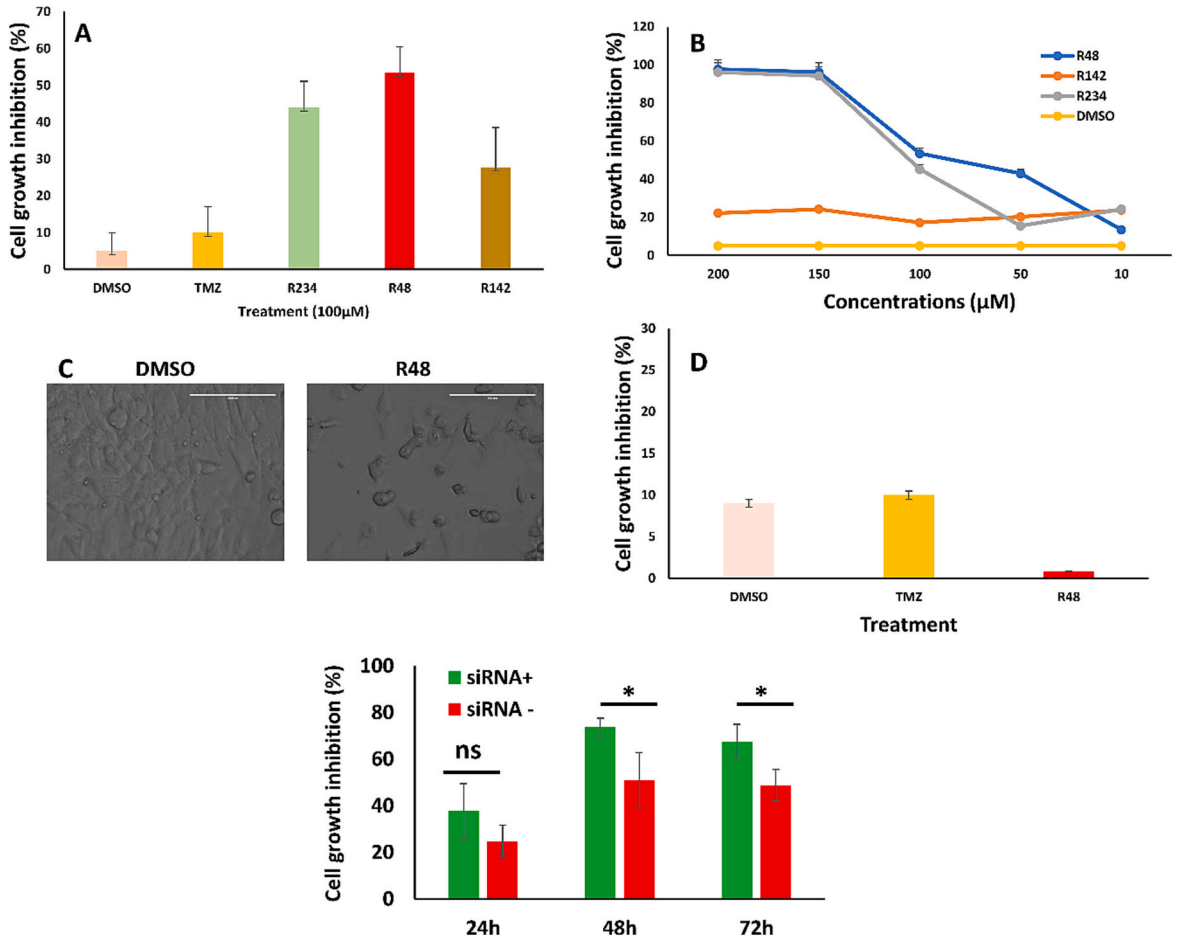

Fig. 5. TrkA targeting novel hydrazone induced cell death in GBM cells. A) Cytotoxicity assay of R234, R48, R142 in U-87 MG cell line at 100 μM concentration. Live and dead cell percentage was measured by the Trypan Blue exclusion method. B) Dose dependant cytotoxicity analysis of R234, R48, R142 with varying concentration of 10 μM, 50 μM, 100 μM, 150 μM and 200 μM for 24 h C) Phase contrast image of U-87 MG cells treated with DMSO and R48. D) Cell growth inhibition of R48 and TMZ in TrkA expressing MEF cells line. E) R48-TrkA-specific siRNA induced cytotoxicity assay for varying time, 24 h, 48 h and 72 h and cell growth inhibition (%) was analysed using trypan blue assay. Datapoints and error bars represent mean ± S.E.M ($n = 4$ per group). *$P < 0.05$ per one-way ANOVA.

than the untreated cells (Fig. 5C). Thus, R48 being the top lead compound was tested for its effect on the TrkA expressing normal cell line, MEF. R48 showed <1 % cell growth inhibition than the TMZ (Fig. 5D), which indicated the specific cytotoxicity activity of R48 in the GBM cells. R48, the top lead compound was tested for its effect on MEF, a normal cell line expressing TrkA, and showed <1 % cell growth inhibition compared to TMZ (Fig. 5D). This data suggest that R48 exerts specific cytotoxicity to only GBM cells. However, the specificity of R48 targeting TrkA in GBM cells needs to be validated and hence, further SiRNA analysis was performed.

3.5. SiRNA assay uncovers off-target effect of R48 induced cytotoxicity

TrkA-specific SiRNA assay was employed to investigate the specificity of R48 binding to the TrkA receptor as described in method section. Cells were exposed to 200 μM of R48 for 48 h after SiRNA transfection for varying time, 24 h, 48 h and 72 h. There observed a greater cytotoxicity by TrkA-specific SiRNA than the R48-TrkA-specific SiRNA in U-87 MG cells. Prolonged transfection of SiRNA also showed similar trend in exerting cytotoxicity (Fig. 5E). This might be due to the off-target activity of R48 in inducing the GBM cell death, thus warrants further empirical investigation.

4. Discussion

Cancer treatment remains a major health problem worldwide, which demands screening of novel bioactive compounds and investigation on their mechanism of action. Among several impediments in developing cancer treatment, drug resistance is the major obstacle. To overcome this challenge, many research groups have developed potential synthetic compounds using advanced strategies. Notably, sixteen coumarin hydrazide–hydrazone derivatives were synthesized that have shown potent anti-tumor activity against pancreatic carcinoma cells and hepatic carcinoma cells. These derivatives have also induced apoptosis via caspase 3/7 and cell cycle arrest. Similarly, novel synthetic quinoline hydrazones showed higher cytotoxicity on human promyelocytic leukemia, breast cancer cells and prostate cancer cells. These derivatives were also identified as a potent EGFR inhibitor [44]. Specifically, compound (*E*)-N′-((2-(4-fluorophenoxy)quinolin-3-yl)methylene)-2-(2-methyl-5-nitro-1H-imidazol-1-yl)acetohydrazide showed EGFR pathway inhibitory activities through EGFR/HER-2 kinases inhibition. This analog has induced cytotoxicity against the growth of adenocarcinoma human alveolar basal epithelial and liver cancer cells. Recently, we have synthesized and evaluated the biological activity of 23 arylhydrazones of active methylene compounds (AHAMCs) against the growth of GBM cell lines. Compound R234, 2-(2-(2,4-dioxopentan-3-ylidene)hydrazineyl)benzonitrile, was identified as EGFR inhibitor. R234 was found to be a negative modulator of RTKs (NGFR), which also

affected the PI3K/AKT/mTOR signaling pathway in GBM cells [19].

NGF has been found to promote either mitogenesis or differentiation and maintenance, depending on how the cell line interacting with TrkA receptors [45]. The biological and pharmacodynamics characteristics of the hydrazone derivative under evaluation shown their versatility in the anti-GBM behavior via tyrosine kinase (TrKA) inhibition. Among the studied analogs, R48 acyl derivatives expressed better anti-GBM activity. Compound R48 showed most effective inhibition (IC_{50} = 68.99 μM) by binding into the active pocket of TrkA receptor with minimum binding energy (−7.62 kcal/mol). It was also observed that the IC_{50} value of R234 was calculated as 107 μM in U8 while it is lower, 68.99 μM, for R48 compound suggesting that R48 as potential compound in inhibiting GBM. Additionally, in-silico analysis suggests that the binding energy between TrkA and selected compounds was −7.62, −8.14, and −8.98 kcal/mol for R48, R142, and R234, respectively. This free energy and the magnitude of the binding affinity between the TrkA- R48 suggest the direct interaction potency of the compound than the known TrkA inhibitor R234. R48 was identified to have interactions with hydrophobic residues, Ile, Phe, Leu, Ala, and Val residues of TrkA. Comparatively, the in-silico analysis revealed that among all the tested compounds, R48 had stronger and stable interaction between the TrkA. However, in-vitro analysis has shown the off-target effect of R48 with TrkA receptor in inducing the GBM cell death. This challenge with selectivity could be attributed to TrkA's strong homology with TrkB and TrkC in the ATP binding site, or due to mutations in the ATP active site [46]. Based on our findings, R48 is thought to have intriguing in-silico interactions with TrkA, but more structural alterations of R48 are needed to prove its potential as a TrkA inhibitor, with significant implications for future GBM therapeutics.

Abbreviations

NGF	Nerve growth factor
TrkA	Tropomyosin kinase receptor kinase type A
GBM	Glioblastoma or Glioblastoma multiforme
RTKs	receptor tyrosine kinases
EGFR	Epidermal growth factor receptors
AHAMCs	Arylhydrazones of active methylene compounds

CRediT authorship contribution statement

A.V.G and K.T.M synthesized and characterized the compounds; A. M, K.S and K.J executed the experiments. S.K, performed siRNA analysis and data validation. K.S, performed computational analysis. A.M and T. R performed data analysis. M.K conceived and managed all studies. A.V. G, K.T.M, AM, K.S, K.J, T.R, and M.K revised the manuscript. All the authors did the technical revision and discussion. All the authors contributed to writing the manuscript.

Funding

This work has been supported by the Fundação para a Ciência e a Tecnologia (FCT) (Portugal), projects UIDB/00100/2020 and UIDP/00100/2020 of Centro de Química Estrutural, and LA/P/0056/2020 of Institute of Molecular Sciences. A.V.G. and K.T.M. thank FCT and Instituto Superior Técnico (DL 57/2016 and L 57/2017 Programs, Contracts no: IST-ID/110/2018 and IST-ID/85/2018), as well as Baku State University (Azerbaijan). Authors thank the Portuguese NMR Network (IST-UL Centre) and the IST Node of the Portuguese Network of mass-spectrometry.

Declaration of competing interest

The authors declare no conflict of interest.

References

[1] G. Mutharasu, A. Murugesan, S. Konda Mani, O. Yli-Harja, M. Kandhavelu, Transcriptomic analysis of glioblastoma multiforme providing new insights into GPR17 signaling communication, J. Biomol. Struct. Dyn. 40 (2022) 2586–2599, https://doi.org/10.1080/07391102.2020.1841029/SUPPL_FILE/TBSD_A_1841029_SM0897.XLS.

[2] P. Nguyen, P. Doan, T. Rimpilainen, S. Konda Mani, A. Murugesan, O. Yli-Harja, N. R. Candeias, M. Kandhavelu, Synthesis and preclinical validation of novel indole derivatives as a GPR17 agonist for glioblastoma treatment, J. Med. Chem. 64 (2021) 10908–10918, https://doi.org/10.1021/ACS.JMEDCHEM.1C00277/SUPPL_FILE/JM1C00277_SI_003.CSV.

[3] A. Mirshafiey, G. Ghalamfarsa, B. Asghari, G. Azizi, Receptor tyrosine kinase and tyrosine kinase inhibitors, Innov, Clin. Neurosci. 11 (2014) 23–36.

[4] D.R. Robinson, Y.-M. Wu, S.-F. Lin, The protein tyrosine kinase family of the human genome, Oncogene 19 (2000) 5548–5557, https://doi.org/10.1038/sj.onc.1203957.

[5] M.K. Paul, A.K. Mukhopadhyay, Tyrosine kinase – role and significance in cancer, Int. J. Med. Sci. 1 (2004) 101–115.

[6] E. Carrasco-García, M. Saceda, I. Martínez-Lacaci, Role of receptor tyrosine kinases and their ligands in glioblastoma, Cells 3 (2014) 199–235, https://doi.org/10.3390/cells3020199.

[7] H.S. Singer, B. Hansen, D. Martinie, C.L. Karp, Mitogenesis in glioblastoma multiforme cell lines: a role for NGF and its TrkA receptors, J. Neurooncol 45 (1999) 1–8, https://doi.org/10.1023/a:1006323523437.

[8] M.I.D. Silva, B.W. Stringer, C. Bardy, Neuronal and tumourigenic boundaries of glioblastoma plasticity, Trends in Cancer. 9 (2023) 223–236, https://doi.org/10.1016/j.trecan.2022.10.010.

[9] Y. Wang, C. Hagel, W. Hamel, S. Müller, L. Kluwe, M. Westphal, Trk A, B, and C are commonly expressed in human astrocytes and astrocytic gliomas but not by human oligodendrocytes and oligodendroglioma, Acta Neuropathol. 96 (1998) 357–364, https://doi.org/10.1007/s004010050906.

[10] L.A. Hutton, J. deVellis, J.R. Perez-Polo, Expression of p75NGFR TrkA, and TrkB mRNA in rat C6 glioma and type I astrocyte cultures, J. Neurosci. Res. 32 (1992) 375–383, https://doi.org/10.1002/jnr.490320309.

[11] R.M. Lindsay, S.J. Wiegand, C.A. Altar, P.S. DiStefano, Neurotrophic factors: from molecule to man, Trends Neurosci. 17 (1994) 182–190, https://doi.org/10.1016/0166-2236(94)90099-x.

[12] S. Kumar, L.A. Peña, J. de Vellis, CNS glial cells express neurotrophin receptors whose levels are regulated by NGF, Brain Res. Mol. Brain Res. 17 (1993) 163–168, https://doi.org/10.1016/0169-328x(93)90086-5.

[13] A. Junghänel, A. Berndt, H. Kosmehl, P. Hyckel, Cell kinetics of oral squamous epithelial carcinomas. Determination of the proliferation index and apoptosis rate with the TUNEL method, Mund Kiefer Gesichtschir. 2 (1998) 250–255, https://doi.org/10.1007/s100060050069.

[14] R. McLendon, A. Friedman, D. Bigner, E.G. Van Meir, D.J. Brat, G. M. Mastrogianakis, J.J. Olson, T. Mikkelsen, N. Lehman, K. Aldape, W.K. Alfred Yung, O. Bogler, S. VandenBerg, M. Berger, M. Prados, D. Muzny, M. Morgan, S. Scherer, A. Sabo, L. Nazareth, L. Lewis, O. Hall, Y. Zhu, Y. Ren, O. Alvi, J. Yao, A. Hawes, S. Jhangiani, G. Fowler, A. San Lucas, C. Kovar, A. Cree, H. Dinh, J. Santibanez, V. Joshi, M.L. Gonzalez-Garay, C.A. Miller, A. Milosavljevic, L. Donehower, D.A. Wheeler, R.A. Gibbs, K. Cibulskis, C. Sougnez, T. Fennell, S. Mahan, J. Wilkinson, L. Ziaugra, R. Onofrio, T. Bloom, R. Nicol, K. Ardlie, J. Baldwin, S. Gabriel, E.S. Lander, L. Ding, R.S. Fulton, M.D. McLellan, J. Wallis, D.E. Larson, X. Shi, R. Abbott, L. Fulton, K. Chen, D.C. Koboldt, M. C. Wendl, R. Meyer, Y. Tang, L. Lin, J.R. Osborne, B.H. Dunford-Shore, T.L. Miner, K. Delehaunty, C. Markovic, G. Swift, W. Courtney, C. Pohl, S. Abbott, A. Hawkins, S. Leong, C. Haipek, H. Schmidt, M. Wiechert, T. Vickery, S. Scott, D.J. Dooling, A. Chinwalla, G.M. Weinstock, E.R. Mardis, R.K. Wilson, G. Getz, W. Winckler, R.G. W. Verhaak, M.S. Lawrence, M. O'Kelly, J. Robinson, G. Alexe, R. Beroukhim, S. Carter, D. Chiang, J. Gould, S. Gupta, J. Korn, C. Mermel, J. Mesirov, S. Monti, H. Nguyen, M. Parkin, M. Reich, N. Stransky, B.A. Weir, L. Garraway, T. Golub, M. Meyerson, L. Chin, A. Protopopov, J. Zhang, I. Perna, S. Aronson, N. Sathiamoorthy, G. Ren, J. Yao, W.R. Wiedemeyer, H. Kim, S. Won Kong, Y. Xiao, I.S. Kohane, J. Seidman, P.J. Park, R. Kucherlapati, P.W. Laird, L. Cope, J. G. Herman, D.J. Weisenberger, F. Pan, D. Van Den Berg, L. Van Neste, J. Mi Yi, K. E. Schuebel, S.B. Baylin, D.M. Absher, J.Z. Li, A. Southwick, S. Brady, A. Aggarwal, T. Chung, G. Sherlock, J.D. Brooks, R.M. Myers, P.T. Spellman, E. Purdom, L. R. Jakkula, A.V. Lapuk, H. Marr, S. Dorton, Y. Gi Choi, J. Han, A. Ray, V. Wang, S. Durinck, M. Robinson, N.J. Wang, K. Vranizan, V. Peng, E. Van Name, G. V. Fontenay, J. Ngai, J.G. Conboy, B. Parvin, H.S. Feiler, T.P. Speed, J.W. Gray, C. Brennan, N.D. Socci, A. Olshen, B.S. Taylor, A. Lash, N. Schultz, B. Reva, Y. Antipin, A. Stukalov, B. Gross, E. Cerami, W. Qing Wang, L.-X. Qin, V.E. Seshan, L. Villafania, M. Cavatore, L. Borsu, A. Viale, W. Gerald, C. Sander, M. Ladanyi, C. M. Perou, D. Neil Hayes, M.D. Topal, K.A. Hoadley, Y. Qi, S. Balu, Y. Shi, J. Wu, R. Penny, M. Bittner, T. Shelton, E. Lenkiewicz, S. Morris, D. Beasley, S. Sanders, A. Kahn, R. Sfeir, J. Chen, D. Nassau, L. Feng, E. Hickey, J. Zhang, J.N. Weinstein, A. Barker, D.S. Gerhard, J. Vockley, C. Compton, J. Vaught, P. Fielding, M. L. Ferguson, C. Schaefer, S. Madhavan, K.H. Buetow, F. Collins, P. Good, M. Guyer, B. Ozenberger, J. Peterson, E. Thomson, The Cancer Genome Atlas Research Network, Tissue source sites: Duke University Medical School, Emory University, Henry Ford Hospital, MD Anderson Cancer Center, University of California San Francisco, Genome sequencing centres: Baylor College of Medicine, Broad Institute of MIT and Harvard, Washington University in St Louis, Cancer genome characterization centres: Broad Institute/Dana-Farber Cancer Institute, Harvard Medical School/Dana-Farber Cancer Institute, Johns Hopkins/University of

Southern California, HudsonAlpha Institute/Stanford University, Lawrence Berkeley National Laboratory, Memorial Sloan-Kettering Cancer Center, C.H. University of North Carolina, Biospecimen Core Resource, Data Coordinating Center, Project teams: National Cancer Institute, National Human Genome Research Institute, Comprehensive genomic characterization defines human glioblastoma genes and core pathways, Nature 455 (2008) 1061–1068, https://doi.org/10.1038/nature07385.

[15] A. Qin, A. Musket, P.R. Musich, J.B. Schweitzer, Q. Xie, Receptor tyrosine kinases as druggable targets in glioblastoma: do signaling pathways matter? Neuro-Oncology Advances 3 (2021), vdab133 https://doi.org/10.1093/noajnl/vdab133.

[16] H.K. Brar, J. Jose, Z. Wu, M. Sharma, Tyrosine kinase inhibitors for glioblastoma multiforme: challenges and opportunities for drug delivery, Pharmaceutics 15 (2023) 59, https://doi.org/10.3390/pharmaceutics15010059.

[17] T. Regad, Targeting RTK signaling pathways in cancer, Cancers (Basel). 7 (2015) 1758–1784, https://doi.org/10.3390/cancers7030860.

[18] S.J. Miknyoczki, H. Chang, A. Klein-Szanto, C.A. Dionne, B.A. Ruggeri, The Trk tyrosine kinase inhibitor CEP-701 (KT-5555) exhibits significant antitumor efficacy in preclinical xenograft models of human pancreatic ductal adenocarcinoma1, Clin. Cancer Res. 5 (1999) 2205–2212.

[19] A. Viswanathan, D. Kute, A. Musa, S. Konda Mani, V. Sipilä, F. Emmert-Streib, F. I. Zubkov, A.V. Gurbanov, O. Yli-Harja, M. Kandhavelu, 2-(2-(2,4-dioxopentan-3-ylidene)hydrazineyl)benzonitrile as novel inhibitor of receptor tyrosine kinase and PI3K/AKT/mTOR signaling pathway in glioblastoma, Eur. J. Med. Chem. 166 (2019), https://doi.org/10.1016/j.ejmech.2019.01.021.

[20] S. Rollas, Ş. Güniz Küçükgüzel, Biological activities of hydrazone derivatives, Molecules 12 (2007) 1910–1939, https://doi.org/10.3390/12081910.

[21] R. Narang, B. Narasimhan, S. Sharma, A review on biological activities and chemical synthesis of hydrazide derivatives, Curr. Med. Chem. 19 (2012) 569–612, https://doi.org/10.2174/092986712798918789.

[22] V.J. Negi, Biological activities of hydrazone derivatives in the new millennium, Int J Pharmceut Chem. 2 (2013) 100–109, https://doi.org/10.7439/ijpc.v2i4.516.

[23] G. Xu, M.C. Abad, P.J. Connolly, M.P. Neeper, G.T. Struble, B.A. Springer, S. L. Emanuel, N. Pandey, R.H. Gruninger, M. Adams, S. Moreno-Mazza, A.R. Fuentes-Pesquera, S.A. Middleton, 4-Amino-6-arylamino-pyrimidine-5-carbaldehyde hydrazones as potent ErbB-2/EGFR dual kinase inhibitors, Bioorg. Med. Chem. Lett. 18 (2008) 4615–4619, https://doi.org/10.1016/j.bmcl.2008.07.020.

[24] S.M. Abou-Seri, Synthesis and biological evaluation of novel 2,4′-bis substituted diphenylamines as anticancer agents and potential epidermal growth factor receptor tyrosine kinase inhibitors, Eur. J. Med. Chem. 45 (2010) 4113–4121, https://doi.org/10.1016/j.ejmech.2010.05.072.

[25] A.G. Robertson, M.J. Banfield, S.J. Allen, J.A. Dando, G.G. Mason, S.J. Tyler, G. S. Bennett, S.D. Brain, A.R. Clarke, R.L. Naylor, G.K. Wilcock, R.L. Brady, D. Dawbarn, Identification and structure of the nerve growth factor binding site on TrkA, Biochem. Biophys. Res. Commun. 282 (2001) 131–141, https://doi.org/10.1006/bbrc.2001.4462.

[26] H.M. Berman, J. Westbrook, Z. Feng, G. Gilliland, T.N. Bhat, H. Weissig, I. N. Shindyalov, P.E. Bourne, The protein data bank, Nucleic Acids Res. (2000), https://doi.org/10.1093/nar/28.1.235.

[27] R. Huey, G.M. Morris, S. Forli, Using AutoDock 4 and AutoDock Vina with AutoDockTools: A Tutorial, The Scripps Research Institute Molecular, 2012.

[28] G.A. Kaminski, R.A. Friesner, J. Tirado-Rives, Evaluation and reparametrization of the OPLS-AA force field for proteins via comparison with accurate quantum chemical calculations on peptides† –, The Journal of Physical Chemistry B (ACS Publications), The Journal of … 105 (2001) 6474–6487.

[29] D. Seeliger, B.L. de Groot, Ligand docking and binding site analysis with PyMOL and Autodock/Vina, J. Comput. Aided Mol. Des. 24 (2010) 417–422, https://doi.org/10.1007/s10822-010-9352-6.

[30] O. Trott, A.J. Olson, AutoDock Vina: improving the speed and accuracy of docking with a new scoring function, efficient optimization, and multithreading, J. Comput. Chem. (2009), https://doi.org/10.1002/jcc.21334. NA-NA.

[31] B. Hess, C. Kutzner, D. Van Der Spoel, E. Lindahl, GRGMACS 4: algorithms for highly efficient, load-balanced, and scalable molecular simulation, J. Chem. Theory Comput. 4 (2008) 435–447, https://doi.org/10.1021/ct700301q.

[32] W.L. Jorgensen, D.S. Maxwell, J. Tirado-Rives, Development and testing of the OPLS all-atom force field on conformational energetics and properties of organic liquids, J. Am. Chem. Soc. 118 (1996) 11225–11236, https://doi.org/10.1021/ja9621760.

[33] U. Essmann, L. Perera, M.L. Berkowitz, T. Darden, H. Lee, L.G. Pedersen, A smooth particle mesh Ewald method, J. Chem. Phys. (1995), https://doi.org/10.1063/1.470117.

[34] W.L. Jorgensen, J. Chandrasekhar, J.D. Madura, R.W. Impey, M.L. Klein, Comparison of simple potential functions for simulating liquid water, J. Chem. Phys. 79 (1983) 926–935, https://doi.org/10.1063/1.445869.

[35] H.J.C. Berendsen, J.P.M. Postma, W.F. van Gunsteren, J. Hermans, in: B. Pullman (Ed.), Interaction Models for Water in Relation to Protein Hydration BT - Intermolecular Forces: Proceedings of the Fourteenth Jerusalem Symposium on Quantum Chemistry and Biochemistry Held in Jerusalem, Israel, April 13–16, 1981, Springer Netherlands, Dordrecht, 1981, pp. 331–342, https://doi.org/10.1007/978-94-015-7658-1_21.

[36] D. Van Der Spoel, E. Lindahl, B. Hess, G. Groenhof, A.E. Mark, H.J.C. Berendsen, GROMACS: fast, flexible, and free, J. Comput. Chem. 26 (2005) 1701–1718, https://doi.org/10.1002/jcc.20291.

[37] D.E.V. Pires, T.L. Blundell, D.B. Ascher, pkCSM: predicting small-molecule pharmacokinetic and toxicity properties using graph-based signatures, J. Med. Chem. 58 (2015) 4066–4072, https://doi.org/10.1021/acs.jmedchem.5b00104.

[38] K.T. Mahmudov, M.N. Kopylovich, A.J.L. Pombeiro, Coordination chemistry of arylhydrazones of methylene active compounds, Coord. Chem. Rev. 257 (2013) 1244–1281, https://doi.org/10.1016/j.ccr.2012.12.016.

[39] K.T. Mahmudov, M.F.C. Guedes da Silva, M. Glucini, M. Renzi, K.C.P. Gabriel, M. N. Kopylovich, M. Sutradhar, F. Marchetti, C. Pettinari, S. Zamponi, A.J. L. Pombeiro, Water-soluble heterometallic copper(II)-sodium complex comprising arylhydrazone of barbituric acid as a ligand, Inorg. Chem. Commun. 22 (2012) 187–189, https://doi.org/10.1016/j.inoche.2012.06.008.

[40] K.T. Mahmudov, M.N. Kopylovich, A.M. Maharramov, M.M. Kurbanova, A. V. Gurbanov, A.J.L. Pombeiro, Barbituric acids as a useful tool for the construction of coordination and supramolecular compounds, Coord. Chem. Rev. 265 (2014) 1–37, https://doi.org/10.1016/j.ccr.2014.01.002.

[41] T. Geetha, M.L. Seibenhener, L. Chen, K. Madura, M.W. Wooten, p62 serves as a shuttling factor for TrkA interaction with the proteasome, Biochem. Biophys. Res. Commun. 374 (2008) 33–37, https://doi.org/10.1016/j.bbrc.2008.06.082.

[42] S. Giraud, E. Loum, B. Bessette, M. Mathonnet, F. Lalloué, P75 neurotrophin receptor is sequestered in the Golgi apparatus of the U-87 MG human glioblastoma cell line, Int. J. Oncol. 38 (2011) 391–399, https://doi.org/10.3892/ijo.2010.862.

[43] S. Kari, K. Subramanian, I.A. Altomonte, A. Murugesan, O. Yli-Harja, M. Kandhavelu, Programmed cell death detection methods: a systematic review and a categorical comparison, Apoptosis 27 (2022) 482–508, https://doi.org/10.1007/s10495-022-01735-y.

[44] A. Martorana, G. La Monica, A. Lauria, Quinoline-based molecules targeting c-Met, EGF, and VEGF receptors and the proteins involved in related carcinogenic pathways, Molecules 25 (2020) 4279, https://doi.org/10.3390/molecules25184279.

[45] T. Toni, P. Dua, P.H. van der Graaf, Systems pharmacology of the NGF signaling through p75 and TrkA receptors, CPT Pharmacometrics Syst. Pharmacol. 3 (2014), e150, https://doi.org/10.1038/psp.2014.48.

[46] X. Wu, Q. Li, S. Wan, J. Zhang, Molecular dynamics simulation and free energy calculation studies of the binding mechanism of allosteric inhibitors with TrkA kinase, Journal of Biomolecular Structure and Dynamics. 39 (2021) 202–208, https://doi.org/10.1080/07391102.2019.1708798.